Development of Theoretical Foundations of the Controlled Synthesis of Multifunctional Coatings by the Micro-Arc Oxidation Method

Pavel Golubkov, Ekaterina Pecherskaya, Oleg Karpanin, Maxim Safronov,
Timur Zinchenko, Dmitriy Artamonov
Penza State University
Penza, Russia
golpavpnz@yandex.ru, pea1@list.ru

***Abstract*—A methodology for the controlled synthesis of protective coatings by the micro-arc oxidation method, including a mathematical model of a galvanic cell based on an equivalent electrical circuit, as well as a model of the interconnections between the technological parameters of the micro-arc oxidation (MAO) process and the properties of the obtained oxide layers based on graph theory has been developed. The indicated dependences are formalized using methods of regression and correlation analysis of experimental data. A technique for the controlled synthesis of MAO coatings using the obtained regression equations is proposed. The technique was used in the selection of optimal technological parameters for producing oxide layers with a thickness of 100 μm and a minimum porosity. A prototype of an intelligent automated system for the controlled synthesis of MAO coatings, which was used to obtain experimental dependences of reaction parameters on the influence parameters of the micro-arc oxidation process was created; the principle of the hardware and software of the system is presented.**

I. Introduction

Micro-arc oxidation is a promising and rapidly developing technology that allows plasma-chemical deposition of oxide coatings to give to the surfaces of valve metal and alloy parts high operational characteristics: micro-hardness, wear resistance, corrosion resistance and biocompatibility [1 – 3]. In addition to the traditional fields of this technology application (mechanical engineering, the aerospace, rocket and space industries, prosthetics in medicine), new ones (dosimetry) appear or existing ones (prostheses with antibacterial properties) expand [4, 5], which in the long term can lead to great demand for products with such coatings among citizens not only of Russia, but also of other countries.

It should be noted, however, that in order to successfully obtain multifunctional coatings by the micro-arc oxidation method on an industrial scale, optimal technological conditions must be developed to guarantee high quality of the finished product at the minimum cost of its production, which is associated with some difficulties. Firstly, this is a large number of heterogeneous factors that simultaneously affect the properties of the formed oxide layer [6]; secondly, the variety of possible directions of use, for which the requirements for the properties of the finished coating can vary widely; thirdly, insufficient knowledge of the MAO process, the lack of an analytical description of a number of interconnections between influencing factors; and fourthly, the imperfection of technological and measuring equipment, the inability to control and register the oxide layers properties in the process of their formation. All this greatly complicates the development of the technological process and leads to the need to create an automated system that realizes the production of MAO coatings with the required properties.

Currently, works of this kind are being conducted both in Russia and abroad [7 – 9], in particular, in [10, 11], the concept of an intelligent automated system for the controlled synthesis of MAO coatings, including a description of the structure and functioning algorithm, was proposed but theoretical positions on which the intelligent application of controlled synthesis is based, as well as methods for choosing the optimal technological mode, were not considered. This article proposes theoretical models that make up the methodology for the controlled synthesis of oxide coatings, and also presents the layout structure of an intelligent automated micro-arc oxidation system. In section II of this article an electrophysical model of the oxide layers formation, as well as a model of the relationships between the technological parameters of the MAO process and the properties of MAO coatings based on graph theory was proposed. In section III a method for the controlled synthesis of MAO coatings with desired properties was developed. In section IV the structure and the operation principle of a prototype of an intelligent automated MAO system was described. In section V conclusions on the work, describes the significance of the proposed theoretical models, the possibilities of their use in creating an intelligent automated MAO system were presented.

II. Models used in the development of a methodology for controlled synthesis of MAO-coatings

The intelligent automated controlled synthesis system proposed in [10, 11] is designed to solve two main problems: theoretical (study of the interconnections between the parameters of the MAO process and the properties of the obtained oxide layers) and practical (controlled synthesis of MAO coatings with desired properties for various applications in industry). Accordingly, the mathematical models considered below can also be divided into models for solving theoretical and applied problems. The first model includes the MAO process model based on the equivalent electrical circuit, the

second - based on graph theory.

A. Electrophysical model of the MAO process

As it is known, the MAO process has a pronounced staging. The anodizing stage is characterized by the formation of a dense barrier layer of metal oxide (in this case, aluminum), and then a porous layer. As the anode oxide film thickness increases, the voltage drop on it increases, which leads to its breakdown and the appearance of sparks on the part surface - the sparking stage begins. In this case, the heating of the pore walls (discharge channels) accelerates the electrochemical processes in them, the pore is overgrown with oxide, and breakdown occurs elsewhere. As the coating thickness increases, the power of micro-discharges increases, which contributes to the occurrence of plasma-chemical reactions in the pores and the phase transition of amorphous alumina (γ-Al_2O_3) to the crystalline modification corundum (α-Al_2O_3), i.e., the stage of micro-arc discharges begins. The higher the proportion of corundum in the coating, the better are its mechanical, chemical and electrical characteristics. With an even greater increase in the power of micro-discharges, the coating is destroyed (stage of arc discharges).

The authors proposed the interpretation of the galvanic cell at different stages of the formation of the MAO coating in the form of an equivalent electrical circuit (Fig. 1).

At the stage of formation of the barrier layer, the resistance of the porous layer and micro-discharges $R_{pl} = 0$, $R_{dis} = 0$, respectively, the coating capacity C_{coat} is the coating capacity C_{bl}. For the resulting scheme according to the second Kirchhoff law, we have:

$$U(t) = I(t)R_{el} + \frac{I_1(t)}{\omega C_{bl}} + I_2(t)R_{bl}\,, \tag{1}$$

where ω is the cyclic frequency. Express the voltage drop in section AB, which characterizes all stages of the MAO process from (1):

$$U_{AB}(t) = U(t) - I(t)R_{el} = \frac{I_1(t)}{\omega C_{bl}} + I_2(t)R_{bl}\,, \tag{2}$$

where $I(t) = I_1(t) + I_2(t)$ is the technological current.

At the second stage of the anodizing, the resistance of the porous layer R_{pl}, which is a parallel connection of the resistances of individual pores, as well as the coating capacity C_{coat} in the form of a series connection of the capacitances of the barrier and porous layers, is taken into account. The equation according to the first Kirchhoff law for the contour C_{coat}-R_{bl}-R_{pl} has the form:

$$I(t) = I_1(t) + I_2(t) = U_{AB}(t)\omega C_{coat} + \frac{U_{AB}(t)}{R_{bl} + R_{pl}}\,. \tag{3}$$

Taking into account the possibility of measuring the current, voltage, and capacitance of the coating, we write the expression for determining the resistance of the coating R_{coat}:

$$R_{coat} = R_{bl} + R_{pl} = \frac{U_{AB}(t)}{I(t) - U_{AB}(t)\omega C_{coat}}\,. \tag{4}$$

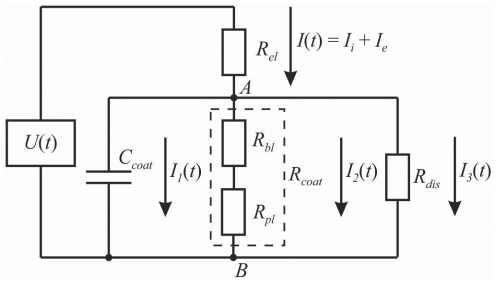

Fig. 1. Equivalent electrical circuit of a galvanic cell

At the stages of micro-discharges (spark, micro-arc, arc) on an equivalent circuit, it is necessary to take into account the resistance of micro-discharges R_{dis}, for which we compose the equation according to the first Kirchhoff law for section AB:

$$I(t) = U_{AB}(t)\omega C_{coat} + \frac{U_{AB}(t)}{R_{coat}} + \frac{U_{AB}(t)}{R_{dis}}\,, \tag{5}$$

where do we find the resistance of micro-discharges R_{dis}:

$$R_{dis} = \frac{U_{AB}(t)R_{coat}}{I(t)R_{coat} - U_{AB}(t)(\omega C_{coat}R_{coat} + 1)}\,. \tag{6}$$

Thus, measuring the current, voltage, and capacitance of the coating during the MAO process allows to determine the resistance of the coating and the resistance of micro-discharges, which can be used to judge the thickness of the coating and the power of micro-discharges, respectively.

There is another approach to the electrophysical description of the MAO process. According to this model, the voltage drop in the galvanic cell at the stage of the barrier layer $U_{F(bl)}(t)$ formation can be determined in the form:

$$U_{F(bl)}(t) = Z_{bl}(t)I(t)\,, \tag{7}$$

$$Z_{bl}(t) = \sqrt{R_b(t)^2 + X_{Cb}(t)^2}\,, \tag{8}$$

$$R_b(t) = R_{bl}(t) + R_{el} = \frac{r_{ox}h_{bl}(t)}{S_{tot}} + R_{el}\,, \tag{9}$$

$$X_{Cb}(t) = \frac{1}{\omega C_{bl}(t)} = \frac{h_{bl}(t)}{\omega\varepsilon_{ox}\varepsilon_0 S_{tot}}\,, \tag{10}$$

where $Z_{bl}(t)$, $R_b(t)$, $X_{Cb}(t)$ is the total, active and reactive resistance of the galvanic cell; $R_{bl}(t)$, $C_{bl}(t)$, $h_{bl}(t)$ - resistance, capacitance and thickness of the barrier layer, respectively; R_{el} is the resistance of the electrolyte between the anode and cathode; r_{ox}, ε_{ox} - resistivity and dielectric constant of the oxide; S_{tot} is the total area of the sample; ω is the cyclic frequency; $I(t)$ is the technological current; ε_0 is the electric constant.

At the stage of formation of the porous layer, the voltage drop in the galvanic cell $U_{F(pl)}(t)$ can be represented as:

$$U_{F(pl)}(t) = \sqrt{(R_p(t) + R_{el})^2 + X_{Cp}(t)^2}\,I(t)\,, \tag{11}$$

$$R_p(t) = R_{bl}(t) + \frac{R_{ep}(t) \cdot R_m(t)}{R_{ep}(t) + R_m(t)}, \quad (12)$$

$$X_{Cp}(t) = \frac{1}{\omega C_{eq}(t)}, \quad (13)$$

where $R_p(t)$, $X_{Cp}(t)$ is the active and reactive resistance of the galvanic cell at the stage of formation of the porous layer. Active resistance is calculated as a series-parallel connection of the resistances of the barrier layer $R_{bl}(t)$, the electrolyte in the pores $R_{ep}(t)$ and the porous oxide matrix $R_m(t)$:

$$R_{ep}(t) = \frac{r_{el} h_{pl}(t)}{S_p(t)}, \quad (14)$$

$$R_m(t) = \frac{r_{ox} h_{pl}(t)}{S_{wp}(t)}. \quad (15)$$

The equivalent capacitance $C_{eq}(t)$ is a series connection of the capacitances of the barrier layer $C_{bl}(t)$ and the oxide matrix $C_m(t)$:

$$C_{eq}(t) = \frac{C_m(t) C_{bl}(t)}{C_m(t) + C_{bl}(t)} = \frac{\varepsilon_{ox} \varepsilon_0 S_{wp}(t) S_{tot}}{S_{wp}(t) h_{pl}(t) + S_{tot} h_{bl}(t)}. \quad (16)$$

In equations (14) - (16), the following notation is adopted: r_{el} - electrolyte resistivity; $h_{pl}(t)$ is the thickness of the porous layer; the total pore area $S_p(t)$ and the area not occupied by the pores $S_{wp}(t)$ are determined based on the Keller model as follows:

$$S_p(t) = \frac{S_{tot} \pi d_p^2(t)}{4 D_{\text{int}}^2(t)}, \quad (17)$$

$$S_{wp}(t) = S_{tot} - S_p(t) = S_{tot} \left(1 - \frac{\pi d_p^2(t)}{4 D_{\text{int}}^2(t)} \right), \quad (18)$$

where $d_p(t)$ is the pore diameter; $D_{int}(t)$ - the distance between the centers of neighboring pores:

$$D_{\text{int}}(t) = k U_F(t), \quad (19)$$

$$d_p(t) = D_{\text{int}}(t) - 1.67 \cdot h_{bl}(t). \quad (20)$$

The thickness of the barrier and porous layers at the anodizing stage can be found according to the Faraday law:

$$h_{bl}(t) = \frac{M_{ox} I(t) t \eta}{z F \rho_{ox} S_{tot}}, \quad (21)$$

$$h_{Pl}(t) = \frac{M_{ox} I(t) t \eta}{z F \rho_{ox} S_{wp}}, \quad (22)$$

where M_{ox}, ρ_{ox} are the molar mass and the oxide density, respectively; z is the number of electrons participating in the oxidation reaction; F - Faraday constant; $I(t)$ is the technological current; t is the oxidation time; η is a coefficient showing the fraction of the current spent on oxidation.

The surface and bulk porosity of the coating $P_S(t)$ and $P_V(t)$ at the anodizing stage is determined as follows:

$$P_S(t) = \frac{S_p(t)}{S_{tot}} = \frac{\pi d_p^2(t)}{4 D_{\text{int}}^2(t)}, \quad (23)$$

$$P_V(t) = \frac{2\pi}{\sqrt{3}} \left(\frac{d_p(t)}{2 D_{\text{int}}(t)} \right)^2. \quad (24)$$

In the subsequent stages of the MAO process, the coating thickness $h(t)$ is determined as follows:

$$h(t) = h_{cr} \exp(k(U_F(t) - U_{cr})), \quad (25)$$

where h_{cr} is the critical thickness of the coating at which breakdown accompanied by a spark discharge occurs; U_{cr} is the sparking voltage (or the voltage of the transition to another discharge type); k - constant. It is known that sparking occurs at a coating thickness h_{cr} from 2 to 2.5 μm, and for small film thicknesses (from 1 to 9 μm) the expression is true:

$$U_{bd} = k_1 h + k_2, \quad (26)$$

where U_{bd} is the breakdown voltage; h is the thickness of the oxide layer; k_1, k_2 are empirical coefficients (for an anodic oxide film obtained in an alkaline electrolyte, $k_1 = 12$, $k_2 = 86$). Thus, to determine of the coating thickness at the stages of micro-discharges, it is necessary to know either the sparking voltage or the critical thickness. Having determined the sparking voltage from the forming curve (Fig. 2) at the end of the anodizing stage, expressing the critical thickness from (26) and substituting the resulting expression in (25), we obtain:

$$h(t) = \frac{U_{cr} - k_2}{k_1} \exp(k(U_F(t) - U_{cr})), \quad (27)$$

Further, sequentially finding the critical stress values at the points of transition of the forming curve to a new stage of

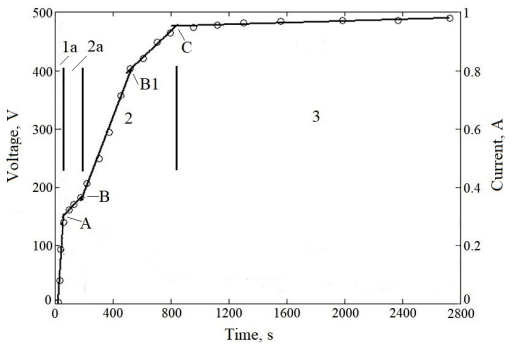

Fig. 2. Forming curve of the MAO process: point *A* - transition to the formation of a porous layer; *B* is the beginning of the spark stage; *C* is the beginning of micro-arc discharges stage; at point *B1*, the ratio of ion and electron currents at the spark stage changes

micro-discharges, using expression (27) we determine the thickness of the coating at these stages.

If we assume that the dielectric breakdown of the oxide layer occurs in all pores, we can obtain the expression for the minimum total current of micro-discharges at the sparking stage [12]:

$$I_{\min}(t) = \frac{P_S I(t) Z_{pl}(t)}{R_{bl}(t) + R_l(t)}, \quad (28)$$

where $R_l(t)$ is the resistance of the electrolyte layer with thickness $h_{pl}(t)$ and area S_{tot}:

$$R_l(t) = \frac{r_{el} h_{pl}(t)}{S_{tot}}. \quad (29)$$

The minimum micro-discharge current in a single pore is determined as follows:

$$I_{por}(t) = I_{\min}(t) N_p = I_{\min}(t) \frac{4 S_p}{\pi d_p^2}. \quad (30)$$

In the case of a spark breakdown, the electrolyte boils in the pore, while the released amount of heat must exceed the heat of vaporization:

$$Q_p \geq Lm, \quad (31)$$

$$Q_p = I_{por}{}^2 R_{ep} t_p = t_p \frac{U_{cr}{}^2}{R_{ep}}, \quad (32)$$

where t_p is the duration of the current pulse; L is the specific heat of vaporization. Then the minimum volume V_b of the vapor-gas bubble formed in the pore can be determined as follows:

$$V_b = \frac{L \rho_{el}}{Q_p}, \quad (33)$$

where ρ_{el} is the electrolyte density. Expression (33) makes it possible to determine the length of the discharge channel l_d at the beginning of the spark discharges stage:

$$l_d = \frac{4 V_b}{\pi d_p^2}. \quad (34)$$

During the burning of a micro-discharge, plasma-chemical reactions, not only intensifying the oxide growth at the bottom of the pore, but also causing a phase transition of amorphous alumina to corundum at high temperature occur in the bubble. This temperature is reached at the stage of micro-arc discharges, with an increase in the power of which the proportion of the formed corundum increases exponentially. This process is described by the Kolmogorov-Johnson-Mehl-Avrami equation:

$$C_\alpha = 1 - \exp\left(-kt^n\right), \quad (35)$$

where C_α is the fraction of the formed corundum; k is a constant, (at an oxide temperature at the bottom of the pore equal to 1050 ºC $k = 8.5 \cdot 10^{-5}$ s^{-1}), t is the duration of the current pulse (micro-discharge burning time), $n = 2.1$ is the Avrami exponent [13, 14].

The obtained expressions are of great scientific and practical importance, since it is micro-discharges that have the main influence on the formation of high-temperature crystalline modifications of valve metal oxides in the working layer of the MAO coating and provide its high performance characteristics: micro-hardness, wear and corrosion resistance, heat resistance, and electric strength. The obtained expressions make it possible to get closer to understanding the processes occurring in the micro-discharge channel during MAO, which have not been sufficiently studied at present, and to analytically describe them, which is a prerequisite for the flexible control of the micro-discharges effect on the oxide layer during its formation. A more detailed description of the electrophysical model of the MAO process is given in [12, 14].

B. A model of the interconnections of parameters-effects and parameters-reactions of the MAO process based on graph theory

As it is known, any modern information control system includes measuring channels of certain physical quantities, and the best technical solution is usually to use the smallest possible number of measuring transducers, allowing to obtain the maximum information about the measurement object. In the case of a complex multifactor technological process, which is the MAO process, the development of such a technical solution requires the involvement of special scientific approaches, in particular, system analysis, graph theory and set theory.

The factors of the MAO process, which can be divided into parameters-effects and parameters-reactions, taking into account their influence on each other and on the properties of the formed oxide coatings, are shown on the model in the form of an oriented graph (Fig. 3). Explanation of the notation is given in Table 1.

It is advisable to present all the parameters of the MAO process in the form of sets (Fig. 4): parameters-effects (set *V*); parameters-reactions (set *R*); parameters that act both as effects and as reactions (set *VR*).

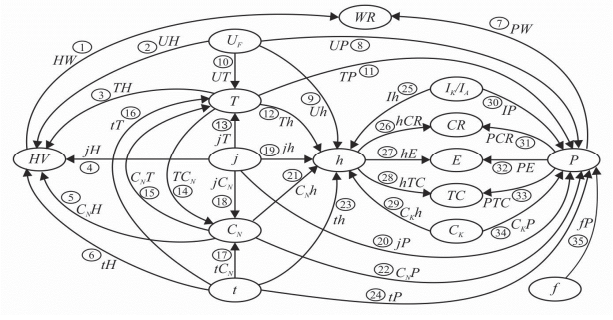

Fig. 3. Oriented graph reflecting the interconnections of the MAO process parameters

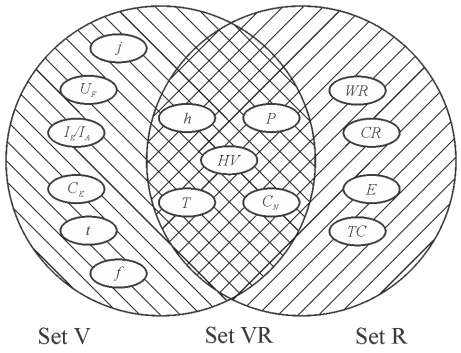

Fig. 4. The distribution of the MAO process parameters by sets

TABLE I. DESIGNATIONS ON THE ORIENTED GRAPH

Designation	Explanation	Designation	Explanation
U_F	Forming voltage	f	Current pulse frequency
T	Electrolyte temperature	C_K	Alkali concentration in the electrolyte
I_K/I_A	Anodic and cathodic currents ratio	C_N	Concentration of sodium silicate in the electrolyte
j	Current density	t	Processing time
h	The oxide layer thickness	P	Porosity of the oxide layer
HV	Micro-hardness	WR	Wear resistance
CR	Corrosion resistance	E	Dielectric strength
TC	Thermal conductivity		

$$V = \{U_F, I_K/I_A, j, C_K, f, t, h, P, HV, T, C_N\}, \quad (36)$$

$$R = \{WR, CR, E, TC, h, P, HV, T, C_N\}, \quad (37)$$

$$VR = \{h, P, HV, T, C_N\}. \quad (38)$$

The interconnections of the parameters-reactions from the parameters-effects shown in Fig. 3, can be described analytically in the form of a system of equations:

$$\begin{cases} \partial WR = HW \cdot \partial HV + PW \cdot \partial P \\ \partial T = UT \cdot \partial U_F + tT \cdot \partial t + C_N T \cdot \partial C_N + jT \cdot \partial j \\ \partial CR = hCR \cdot \partial h + PCR \cdot \partial P \\ \partial HV = UH \cdot \partial U_F + TH \cdot \partial T + jH \cdot \partial j + \\ + C_N H \cdot \partial C_N + tH \cdot \partial t \\ \partial h = Ih \cdot \partial(I_K/I_A) + Uh \cdot \partial U_F + Th \cdot \partial T + \\ + jh \cdot \partial j + C_N h \cdot \partial C_N + th \cdot \partial t + C_K h \cdot \partial C_K \\ \partial E = hE \cdot \partial h + PE \cdot \partial P \\ \partial P = UP \cdot \partial U_F + TP \cdot \partial T + IP \cdot \partial(I_K/I_A) + \\ + C_K P \cdot \partial C_K + jP \cdot \partial j + C_N P \cdot \partial C_N + tP \cdot \partial t + \\ + fP \cdot \partial f \\ \partial C_N = jC_N \cdot \partial j + TC_N \cdot \partial T + tC_N \cdot \partial t \\ \partial TC = hTC \cdot \partial h + PTC \cdot \partial P \end{cases}, \quad (39)$$

where the partial derivatives of HW, PW, etc. (see Table 2) are the properties of the MAO process, which characterize the change in reaction due to a change in a specific effect.

Taking into account the fact that upon the production of MAO coatings in industrial production, it is usually required to stabilize the following technological parameters: T, C_N, C_K, f and assuming the possibility of measuring the parameters-effects and reactions during experiments, we write the system (39) as follows:

TABLE II. MATHEMATICAL DESCRIPTION OF THE MAO PROCESS PROPERTIES

Property	Formula	Property	Formula
th	$th = \frac{\partial h}{\partial t}$	tT	$tT = \frac{\partial T}{\partial t}$
UH	$UH = \frac{\partial HV}{\partial U_F}$	Uh	$Uh = \frac{\partial h}{\partial U_F}$
TH	$TH = \frac{\partial HV}{\partial T}$	Th	$Th = \frac{\partial h}{\partial T}$
jH	$jH = \frac{\partial HV}{\partial j}$	jT	$jT = \frac{\partial T}{\partial j}$
C_NH	$C_N H = \frac{\partial HV}{\partial C_N}$	C_NT	$C_N T = \frac{\partial T}{\partial C_N}$
tH	$tH = \frac{\partial HV}{\partial t}$	tP	$tP = \frac{\partial P}{\partial t}$
PW	$PW = \frac{\partial WR}{\partial P}$	HW	$HW = \frac{\partial WR}{\partial HV}$
UP	$UP = \frac{\partial P}{\partial U_F}$	UT	$UT = \frac{\partial T}{\partial U_F}$
TC_N	$TC_N = \frac{\partial C_N}{\partial T}$	TP	$TP = \frac{\partial P}{\partial T}$
tC_N	$tC_N = \frac{\partial C_N}{\partial t}$	jC_N	$jC_N = \frac{\partial C_N}{\partial j}$
jh	$jh = \frac{\partial h}{\partial j}$	jP	$jP = \frac{\partial P}{\partial j}$
C_Nh	$C_N h = \frac{\partial h}{\partial C_N}$	C_NP	$C_N P = \frac{\partial P}{\partial C_N}$
Ih	$Ih = \frac{\partial P}{\partial t}$	IP	$IP = \frac{\partial P}{\partial I}$
hE	$hE = \frac{\partial E}{\partial h}$	PE	$PE = \frac{\partial E}{\partial P}$
C_Kh	$C_K h = \frac{\partial h}{\partial C_K}$	C_KP	$C_K P = \frac{\partial P}{\partial C_K}$
hCR	$hCR = \frac{\partial CR}{\partial h}$	PCR	$PCR = \frac{\partial CR}{\partial P}$
hTC	$hTC = \frac{\partial TC}{\partial h}$	PTC	$PTC = \frac{\partial TC}{\partial P}$

$$\begin{cases} \partial WR = HW \cdot \partial HV + PW \cdot \partial P \\ \partial CR = hCR \cdot \partial h + PCR \cdot \partial P \\ \partial HV = UH \cdot \partial U_F + jH \cdot \partial j + tH \cdot \partial t \\ \partial h = Ih \cdot \partial (I_K / I_A) + Uh \cdot \partial U_F + jh \cdot \partial j + th \cdot \partial t \\ \partial E = hE \cdot \partial h + PE \cdot \partial P \\ \partial P = UP \cdot \partial U_F + IP \cdot \partial (I_K / I_A) + jP \cdot \partial j + tP \cdot \partial t \\ \partial TC = hTC \cdot \partial h + PTC \cdot \partial P \end{cases} . \quad (40)$$

Analysis (40) shows that the parameters-reactions of the MAO process depend on the forming voltage U_F, current density j, and processing time t. Thus, to determine all the properties of the MAO coatings, it is sufficient to measure the time dependences of the current and voltage, or the dynamic current-voltage characteristics for different values of time.

The transition from (39) to (40) inevitably leads to the appearance of additional errors in the measurement of the MAO process parameters associated with the instability of the parameters T, C_N, C_K, f. This instability is associated mainly with the imperfection of thermostatic control systems, the presence of interference in the supply network and the so-called "degradation", in which the concentration of electrolyte ions irreversibly decreases with prolonged use. Therefore, we assume that each of the stabilized parameters has a region of uncertainty Δ:

$$C_{Nr} \in [C_N - \Delta C_N; C_N + \Delta C_N], \quad (41)$$

$$T_r \in [T - \Delta T; T + \Delta T], \quad (42)$$

$$C_{Kr} \in [C_K - \Delta C_K; C_K + \Delta C_K], \quad (43)$$

$$f_r \in [f - \Delta f; f + \Delta f]. \quad (44)$$

Here C_{Nr}, T_r, C_{Kr}, f_r are real values of stabilized parameters; ΔC_N, ΔT, ΔC_K, Δf are the absolute errors of their stabilization.

The presence of stabilization errors leads to the appearance of additional measurement errors for all other parameters of the system (36). In this case, the deviation of each of the stabilized parameters should be taken into account by introducing an additional term in the corresponding equations of system (37). For example, if the electrolyte temperature is unstable, we have:

$$\partial HV_r = TH \cdot \partial T + UH \cdot \partial U_F + jH \cdot \partial j + tH \cdot \partial t , \quad (45)$$

where ∂HV_r is the relative measurement of micro-hardness due to instability T, a change in U_F, j, t. Then the absolute error of micro-hardness measurements is written as follows:

$$\Delta(\partial HV) = \partial HV_r - \partial HV = TH \cdot \Delta T . \quad (46)$$

Similarly, additional measurement errors of other technological parameters are calculated, for example, thickness h and porosity P:

$$\Delta h = Th \cdot \Delta T = \frac{\partial h}{\partial T} \cdot \Delta T , \quad (47)$$

$$\Delta P = TP \cdot \Delta T = \frac{\partial P}{\partial T} \cdot \Delta T . \quad (48)$$

Thus, a mathematical description of the heterogeneous factors influence on the MAO process allows not only to determine the optimal set of technological parameters measured during processing, but also to take into account additional errors caused by their instability.

C. *Regression and correlation analysis of the empirical laws of the MAO process*

It was previously noted that the properties of the MAO process, which describe physical effects and are expressed through partial derivatives, should be determined experimentally. For this, methods of regression and correlation analysis are used. Correlation analysis is used to establish the presence and type of correlation between the parameters of the MAO process; using regression analysis, analytical expressions that describe the interconnections between parameters-reactions and parameters-effects in the form of regression equations are established. An exponential function is chosen as a single universal form of writing regression equations for the following reasons:

- A single form of regression equations ensures the uniformity and visibility of the graph model, its ease of analysis;
- Many regularities of the MAO process are well approximated by exponential functions;
- Infinite differentiability with conservation of the type of exponential function facilitates mathematical transformations during the study of the MAO process.

The equations obtained in the process of regression and correlation analysis were applied in the development of the methodology for selection the optimal technological parameters for the controlled synthesis of oxide coatings, considered below (see equations (3) - (14) of system (49)).

III. Method for selection the optimal technological parameters of the MAO process

We consider the methodology for selecting the optimal technological mode for producing oxide coatings with desired properties and assign the following requirements to the finished coating:

- Thickness - 100 μm;
- Minimum porosity.

We use the system of equations composed of equations for ∂h and ∂P of systems (39) and the expressions obtained in the course of regression analysis:

$$\begin{cases} \partial h = jh\cdot\partial j + th\cdot\partial t + Ih\cdot\partial(I_K/I_A) + \\ + C_K h\cdot\partial C_K + C_N h\cdot\partial C_N \\ \partial P = UP\cdot\partial U_F + TP\cdot\partial T + IP\cdot\partial(I_K/I_A) + \\ + C_K P\cdot\partial C_K + jP\cdot\partial j + C_N P\cdot\partial C_N + tP\cdot\partial t + \\ + fP\cdot\partial f \\ h(t) = \exp(1{,}29729 + 0{,}0637842\cdot t) \\ h(t) = \exp(1{,}59952 + 0{,}0637521\cdot t) \\ h(I_K/I_A) = \exp(4{,}87429 - 1{,}65459\cdot I_K/I_A) \\ h(I_K/I_A) = \exp(5{,}42726 - 1{,}74454\cdot I_K/I_A) \\ h(C_K) = exp(5{,}17177 - 0{,}152568\cdot C_K) \\ h(C_K) = \exp(5{,}31752 - 0{,}129368\cdot C_K) \\ h(C_K) = \exp(5{,}43303 - 0{,}0982359\cdot C_K) \\ h(C_K) = \exp(5{,}60912 - 0{,}106386\cdot C_K) \\ P(h,j) = \exp(3{,}72041 - 0{,}0164123\cdot h) \\ P(h,j) = \exp(4{,}40629 - 0{,}0156745\cdot h) \\ P(t) = \exp(2{,}41047 - 0{,}00526468\cdot t) \\ P(T) = \exp(0{,}649956 + 0{,}0504057\cdot T) \end{cases} \quad (49)$$

A description of the system (49) regression equations parameters is given in Table. 3.

Technological parameters are determined by the grapho-analytical method. According to the graph of the dependences of the coating thickness on the processing time (equations (3) and (4) of the system (49), Fig. 5), the processing time required to obtain the oxide layer 100 μm is established:

- t = 52 min at a current density of j = 20 A/dm^2.
- t = 47 min at a current density of j = 40 A/dm^2;

Next, the required anodic and cathodic currents ratio is determined using the graph presented in Fig. 6. We have:

- I_K/I_A = 0.16 at a current density of j = 20 A/dm^2;
- I_K/I_A = 0.47 at a current density of j = 40 A/dm^2.

In a first approximation, we have 2 variants of technological regimes for obtaining an MAO coating 100 μm thick.

Option 1:

- current density j = 20 A/dm^2;
- processing time t = 52 min;
- anodic and cathodic currents ratio I_K/I_A = 0.16.

Option 2:

- current density j = 40 A/dm^2;

TABLE III. SYSTEM (49) REGRESSION EQUATIONS PARAMETERS

Equation No.	Parameter-effect	Parameter-reaction	Constant parameter	
			Unit	*Value*
3	Processing time, s	Coating thickness	Current density, A/dm^2	20
4				40
5	Anodic and cathodic currents ratio	Coating thickness	Current density, A/dm^2	20
6				40
7	Concentration of KOH in the electrolyte	Coating thickness	Concentration of Na_2SiO_3, g/l	5
8				10
9				15
10				20
11	Coating thickness	Porosity	Current density, A/dm^2	20
12				40
13	Processing time	Porosity	Current density, A/dm^2	20
14	Electrolyte temperature	Porosity	Current density, A/dm^2	20

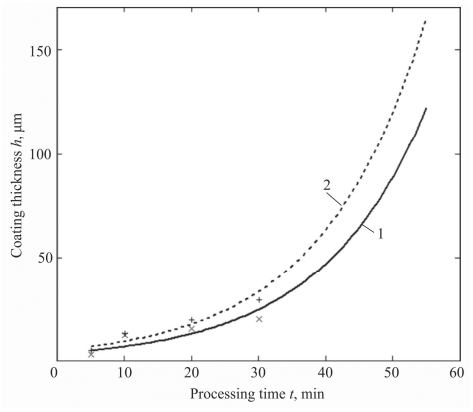

Fig. 5. Dependences of coating thickness on processing time at different current densities: 1 - 20 A/dm^2; 2 - 40 A/dm^2

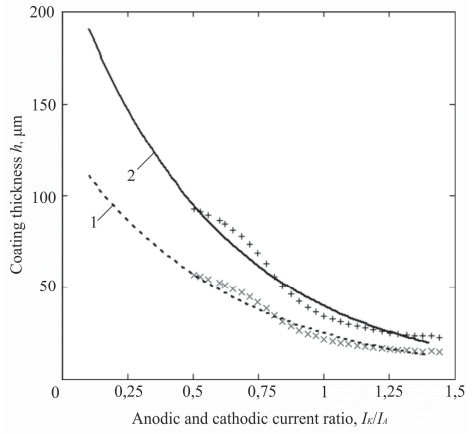

Fig. 6. Dependences of the coating thickness on the ratio of the anode and cathode currents at different current densities: 1 - 20 A/dm^2, 2 - 40 A/dm^2

- processing time t = 47 min;
- anodic and cathodic currents ratio I_K/I_A = 0.47.

To select one of these options, we evaluate the porosity that is obtained with each of them according to Fig. 7:

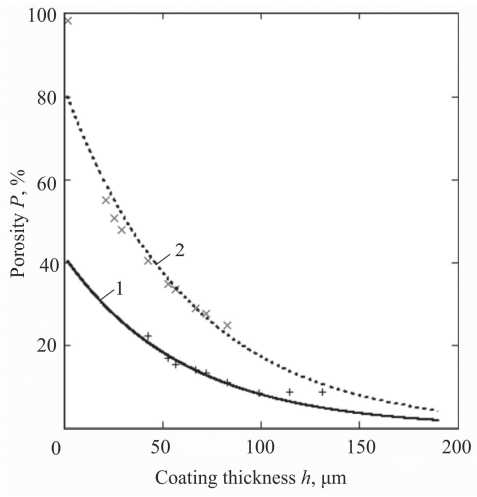

Fig. 7. The dependence of porosity on the thickness of the MAO coating for different current densities: 1 - 20 A/dm^2, 2 - 40 A/dm^2

- P = 8 % at current density j = 20 A/dm^2;
- P = 17 % at current density j = 40 A/dm^2.

It can be seen that the coatings obtained at a current density of 20 A/dm^2 have the minimum porosity (Option 1).

To make sure the selection is correct, according to Fig. 8 we determine the porosity corresponding to the processing time t = 52 min. We obtain the porosity P = 8.5 %, which approximately corresponds to the value obtained previously (8 %). Thus, the technological mode is selected correctly.

Now you should determine the composition of the electrolyte. According to Fig. 9 we select the composition of the electrolyte, in which a coating with a thickness of 100 μm is obtained. We have two options:

- 3.7 g/l KOH and 5 g/l Na_2SiO_3;
- 5.5 g/l KOH and 10 g/l Na_2SiO_3.

These options are equivalent, so you can use any of them.

It is known that when the electrolyte overheats, its dissolving effect is enhanced and the properties of the coating

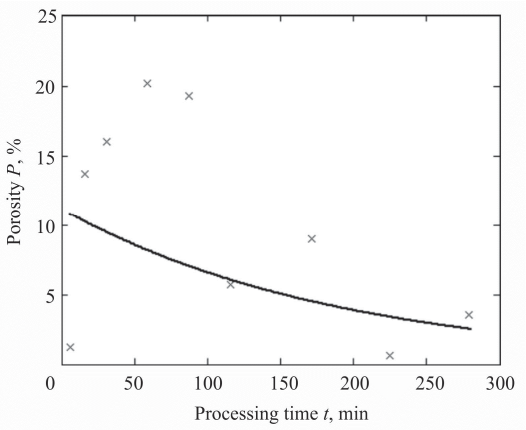

Fig. 8. The dependence of porosity on processing time at a current density of 20 A/dm^2

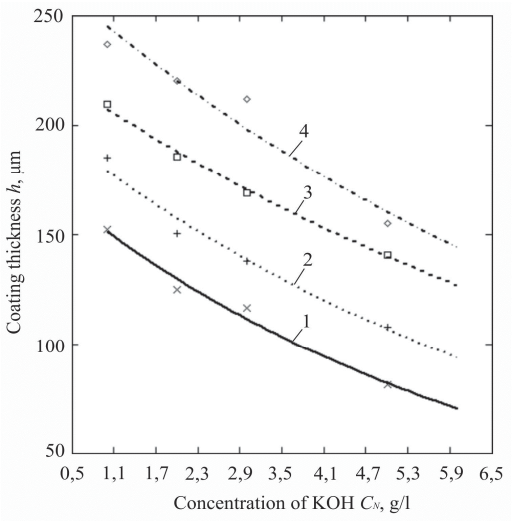

Fig. 9. Dependences of the coating thickness on the concentration of KOH in the electrolyte at a current density of 20 A/dm^2 for a concentration of Na_2SiO_3 equal to: 1 - 5 g/l; 2-10 g/l; 3 - 15 g/l; 4 - 20 g/l

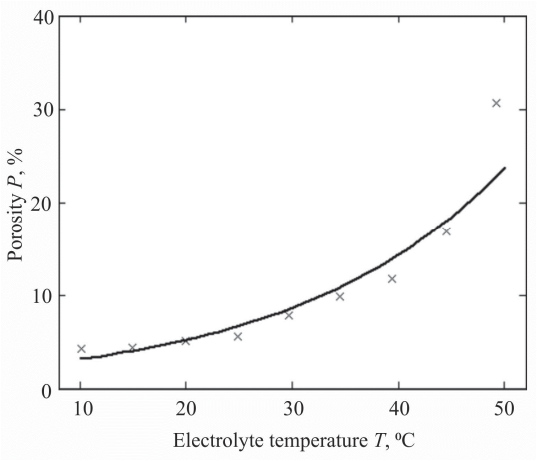

Fig. 10. The dependence of porosity on the temperature of the electrolyte for a current density of 20 A/dm^2

are worsened, in particular, the porosity increases. Let us determine the maximum temperature of the electrolyte at which coatings with desired properties are still obtained. From Fig. 10 it follows that the porosity P = 8.5 % at the maximum electrolyte temperature T = 30 °C.

Thus, to obtain MAO coatings with a thickness of 100 μm and a minimum porosity, it is advisable to use the following technological parameters:

Option 1:

- current density j = 20 A/dm^2;
- processing time t = 52 min;
- anodic and cathodic currents ratio I_K/I_A = 0.16;
- electrolyte composition: 3.7 g/l KOH and 5 g/l Na_2SiO_3.

Option 2:

- current density j = 20 A/dm^2;
- processing time t = 52 min;
- ratio of anode and cathode currents I_K/I_A = 0.16;
- electrolyte composition: 5.5 g/l KOH and 10 g/l Na_2SiO_3.

Thus, the proposed methodology for selecting the optimal technological mode can be considered consistent and used to create an intelligent automated system for the controlled synthesis of MAO coatings.

IV. Development of a Prototype of Intelligent Automated System of Controlled Synthesis of MAO-Coatings

A. Hardware

To obtain experimental data on the interconnections between the parameters-effects and the parameters-reactions of the MAO process, a working model of an intelligent automated system for the controlled synthesis of MAO coatings was designed and assembled, the appearance of which is shown in Fig. 11, the structure is in Figure 12.

The "MAOlab" automated system consists of a technological current source, a galvanic cell, a switching unit,

a measuring board, a power supply unit, a microprocessor module and is connected to a computer via the COM port interface. The technological current source generates a sinusoidal signal with an adjustable current of up to 3 A. The voltage drop across the sample in the galvanic cell can reach up to 400 V.

A galvanic cell is a 1-liter capacity filled with an electrolyte, in which there are two electrodes - an anode and a cathode, and the oxidized part is connected to the anode using a special fastening. The galvanic cell has a protective fence in the form of a magnetic switch - a reed switch.

The measuring board includes a set of measuring transducers of the following values: current and voltage in the galvanic cell, the impedance of the formed coating and the temperature of the electrolyte. The measured impedance values allow to calculate the resistance and capacitance of the coating, which is used to determine the thickness of the oxide layer in real time. However, since the impedance meter is connected to the same contacts as the technological current source, the MAO process has to be interrupted periodically, for which a switch is used.

The microprocessor module is designed for communication with a computer, receiving and transmitting measurement information from sensors, and for ensuring the operation of its hardware in an automated laboratory installation, including for generating warning signals for the operator.

Technical characteristics of the developed device are given in Table. 4.

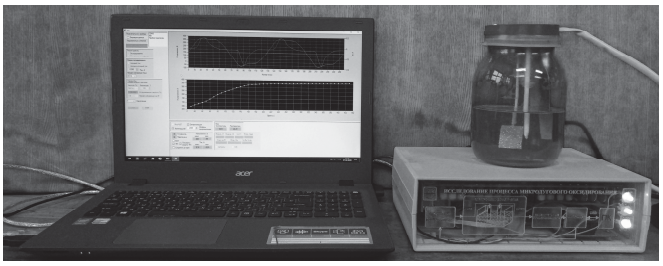

Fig. 11. Automated laboratory installation "MAOlab"

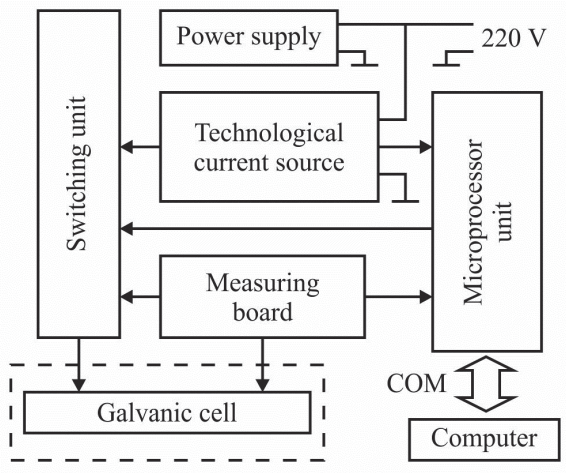

Fig. 12. The structural diagram of the installation "MAOlab"

TABLE IV. TECHNICAL CHARACTERISTICS OF THE "MAOLAB" INSTALLATION

Characteristic	Range
Supply voltage	220 V
The voltage range on the sample	-200 .. +600 V
Range of average current through the sample	0,25 .. 1,75 A
Pulse repetition rate	50 Hz
Frequency range of the test signal	5 Hz .. 10 kHz
The amplitude range of the alternating signal	0,1 .. 1 V
Measurement limits for capacitance	0,1 and 1 μF
The main error in measuring capacitance	not more than 0.5 %
Current measurement limits	0.5 and 3 A
Voltage measurement limit	600 V
The main error in measuring voltage and current	not more than 0.5 %
The number of points for the period	256
Total time of one measurement	no more than 2 s

B. *Software and how to work with it*

The software of the automated system "MAOlab" performs the following functions:

- hardware management;
- receiving, transmitting, processing and displaying measurement information;
- calibration of measuring transducers;
- output of diagnostic messages for the operator.

Data exchange between the installation and the computer is carried out through the COM port in the form of data packets of 256 bytes in size, with the help of which control commands are transmitted and measurement information is entered. The controller, in accordance with the instructions received from the computer, controls the operation of the electronic components of the actuators and measuring transducers of the installation and sends the measurement results to a computer.

The appearance of the program interface is shown in Fig. 13. In this figure, several functional areas can be distinguished:

- connection area;
- area for setting operating modes (oxidation and impedance measurement);
- area of graphic display of signals;
- control area for graphic display of signals;
- area of oxidation parameters;
- area of impedance measurement parameters;
- display area of electrolyte temperature.

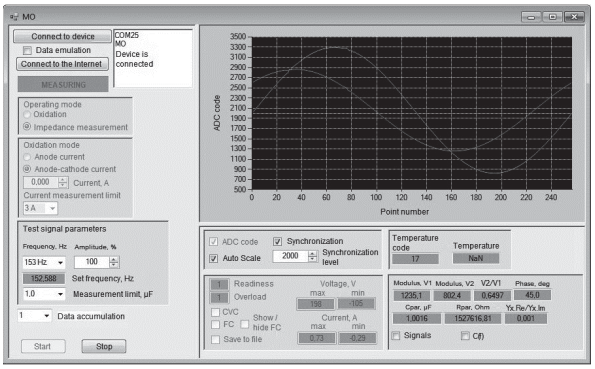

Fig. 13. Appearance of the program interface

To start working with the installation, click the “Connect to the device” button. In this case, the program determines the COM ports connected to the system and sends device identification commands to them. If the identification codes match, the COM port number is saved and data exchange with the installation begins. In this case, the message “Device is connected” is displayed in the message window.

Next, you need to set the operation mode of the device (oxidation or impedance measurement), and the switch is switched over. If the oxidation mode is selected, the parameter settings window is activated (Fig. 14, a), in which the polarity (anode (positive) or anode-cathode (bipolar)), amplitude and measurement limit (0.5 and 3 A) of the technological current are set.

In the impedance measurement mode (Fig. 14, b), the parameters of the sinusoidal input signal of known frequency and amplitude generated by the digital signal synthesizer are adjusted. In the same window, the limit of measuring the capacitance of the formed coating is set (0.1 and 1 μF). The impedance measurement mode allows to obtain the frequency characteristics of a galvanic cell, as well as to evaluate the value of the capacitance and resistance of the coating according to a parallel electrical circuit.

Also, when setting operation modes, it is possible to save and process measurement information. It allows real-time statistical processing of the received data.

The graphical display window of signals allows to display several types of graphs:

In oxidation mode:

- waveforms of current and voltage (Fig. 15, a);
- forming curve (voltage dependency on processing time, Fig. 15, b);
- current-voltage characteristic (Fig. 15, c).

In impedance measurement mode:

- amplitude-frequency and phase-frequency characteristics of a galvanic cell in parallel equivalent electrical circuit (Fig. 15, d).

All obtained dependencies are saved in the form of tables for further processing and analysis.

The window for controlling the graphic display of signals is shown in Fig. 15, e. In this window, you can configure the display of numerical data along the axes in the format “ADC code / measurement unit”, the choice of scale along the axes of

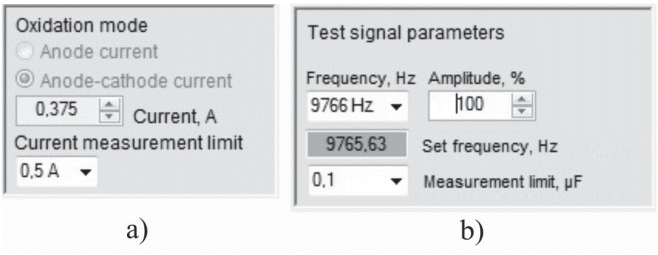

Fig. 14. The window for setting the parameters of the operating modes: a - oxidation; b - impedance measurement

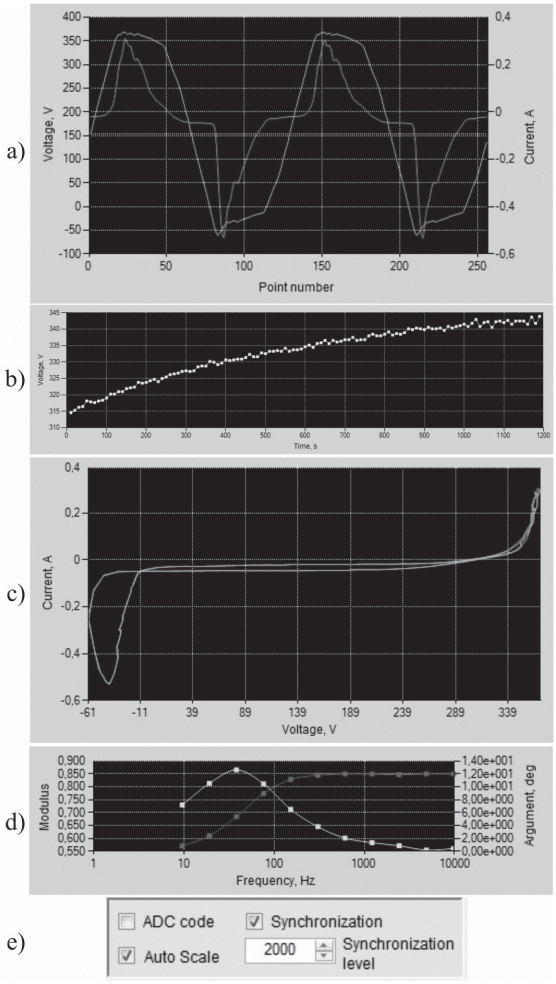

Fig. 15. The window for graphical display of signals: a - waveforms of current and voltage; b - forming curve; c is the current-voltage characteristic; d - frequency characteristics of a galvanic cell; e - a window for controlling the graphic display of signals

the graphs (“Auto Scale”), as well as the synchronization mode at a given level.

The window for displaying oxidation parameters is shown in Fig. 16, a. In this window, the maximum and minimum values of current and voltage in the galvanic cell are displayed, the display of the forming curve and the current-voltage characteristic is regulated. The window for displaying the impedance measurement parameters is shown in Fig. 16, b. This window displays:

- the values of the input and output signals of the measuring impedance transducer and phase shift between them;
- values of the modulus and argument of the complex impedance;
- values of the capacitance and resistance of the coating, calculated according to a parallel equivalent electrical circuit.

Also in the process of oxidation, the electrolyte temperature is measured, the display of which is taken out in a separate window.

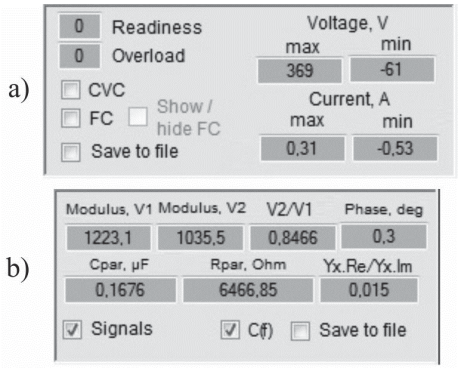

Fig. 16. Window displaying parameters: a - oxidation; b - impedance measurements

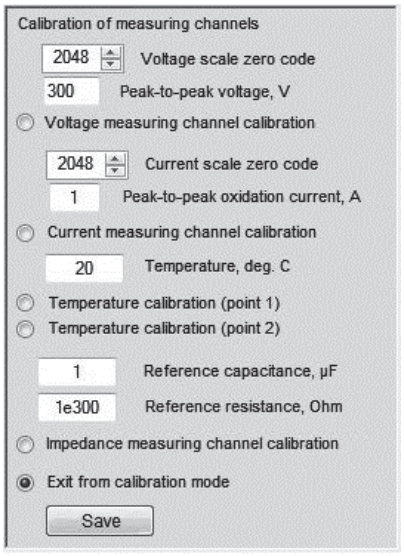

Fig. 17. The window for calibrating measuring instruments

It should be noted that the measurement and display of all technological parameters in the process of coating formation occurs in real time.

The device also has a special set of tools for calibrating measuring instruments (Fig. 17). This window does not appear on the main screen of the program and becomes available only in service mode.

The developed model of the "MAOlab" automated laboratory system is used to conduct experimental studies to identify and analytically describe the dependencies of parameters-reaction on the parameters-effects of the MAO process with the aim of further forming the knowledge base of an intelligent automated system for the synthesis of MAO coatings.

V. Conclusion

Thus, the theoretical positions and practical methods presented in this work that make up the methodology of controlled synthesis are a powerful tool for studying and ensuring the controllability of the MAO process. The obtained regression equations and mathematical models make it possible to predict changes in the properties of oxide coatings in the process of their formation, as well as to take into account their measurement errors caused by the instability of technological factors.

The proposed models will be used in the development of an intelligent application of controlled synthesis of oxide layers and entered into the knowledge base of an intelligent automated system for the controlled synthesis of MAO coatings with a view to further improvement.

Acknowledgment

The reported study was funded by RFBR according to the research project № 19-08-00425.

References

[1] B. Haghighat-Shishavan, R. Azari-Khosrowshahi, S. Haghighat-Shishavan et al., "Improving wear and corrosion properties of alumina coating on AA7075 aluminum by plasma electrolytic oxidation: Effects of graphite absorption", *Appl. Surf. Sci.*, vol. 481, 2019, pp. 108-119.

[2] A. Buling, J. Zerrer, "Increasing the application fields of magnesium by ultraceramic: Corrosion and wear protection by plasma electrolytical oxidation (PEO) of Mg alloys", *Surf. & Coat. Technol.*, vol. 369, 2019, pp. 142-155.

[3] H.F. Nabavi, M. Aliofkhazraei, "Morphology, composition and electrochemical properties of bioactive-TiO2/HA on CP-Ti and Ti6Al4V substrates fabricated by alkali treatment of hybrid plasma electrolytic oxidation process (estimation of porosity from EIS results)", *Surf. & Coat. Technol.*, vol. 375, 2019, pp. 266-291.

[4] J.S. Santos, A. Rodrigues, A.P. Simon et al., "One-Step Synthesis of Antibacterial Coatings by Plasma Electrolytic Oxidation of Aluminum", *Adv. Eng. Mater.*, vol. 21, 2019, pp. 1-6, 1900119.

[5] A. Zolotarjovs, K. Smits, K. Laganovska et al., "Thermostimulated luminescence of plasma electrolytic oxidation coatings on 6082 aluminium surface", *Rad. Meas.*, vol. 124, 2019, pp. 29-34.

[6] P.E. Golubkov, E.A. Pecherskaya, Y.V. Shepeleva et al., "Methods of applying the reliability theory for the analysis of micro-arc oxidation process", *J. of Phys.: Conf. Ser.*, vol. 1124, 2018, pp. 1-6, 081014.

[7] P.E. Golubkov, E.A. Pecherskaya, N.V. Gromkov, T.O. Zinchenko, D.V. Artamonov and I.I. Kochegarov, "Method for Measuring the Oxide Coating Thickness in the Micro-arc Oxidation Process", *in Proc. XXII Int. Conf. on Soft Computing and Measurements (SCM-2019)*, 2019, pp. 204-207.

[8] A.V. Bolshenko, A.V. Pavlenko, V.S. Puzin, I.N. Panenko, "Power Supplies for Microarc Oxidation Devices", *Life Science J.*, vol. 11(1s), 2014, pp. 263-68.

[9] V.N. Borikov, P.F. Baranov, A.D. Bezshlyakh, "Virtual measurement system of electric parameters of microplasma processes", *in Proc. Int. Siberian Conf. on Control and Communications*, 2009, pp. 275-279.

[10] P. Golubkov, E. Pecherskaya, O. Karpanin et al., "Intelligent automated system of controlled synthesis of MAO-coatings", *in Proc. The 24th Conf. of Open Innovations Association FRUCT*, 2019, pp. 96-103.

[11] P.E. Golubkov, E.A. Pecherskaya, O.V. Karpanin et al., "Automation of the micro-arc oxidation process", *J. of Phys.: Conf. Ser.*, vol. 917, 2017, pp. 1-6, 092021.

[12] E.A. Pecherskaya, P.E. Golubkov, D.V. Artamonov, J.V. Shepeleva, "Method for measuring the micro-discharges temperature in the micro-arc oxidation process", *J. of Phys.: Conf. Ser.*, vol. 1393, no 1, 2019, pp. 012083.

[13] V. Dehnavi, X.Y. Liu, B.L. Luan, D.W. Shoesmith, S. Rohani, "Phase transformation in plasma electrolytic oxidation coatings on 6061 aluminum alloy", *Surf. & Coat. Technol.*, vol. 251, 2014, pp. 106-114.

[14] P.E. Golubkov, E.A. Pecherskaya, I.I. Kochegarov, M.I. Safronov and J.V. Shepeleva, "Simulation of Microarc Oxidation Process Based on Equivalent Electric Circuit", *in Proc. XXII Int. Conf. on Soft Computing and Measurements (SCM-2019)*, 2019, pp. 200-203